ES442 Assignment: Scaling of Flexure Mechanisms

Deema Mozayen (U1514864) December 2, 2023

Summary

This report details the analysis of flexure mechanisms in a variety of contexts. Part 1 involves flexure design and considers their motion, materials and dynamics. It was found that the combination of 7075 (T6) alloy and dimensions of 60 x 8.3125 x 0.898 mm proved optimal for the specified leaf-spring mechanism. A notch-hinge equivalent was found to be stiffer yet with more limited deflection. Furthermore, the effect of varying materials and geometric properties was explored extensively in the latter subsections. Part 2 considers flexure fabrication, specifically in the context of Micro Electro-Mechanical Systems (MEMS). A variety of techniques are discussed with micromachining proving the most established and viable method.

Introduction

Flexures refer to a variety of mechanisms that produce motion due to elastic deformation. They present numerous advantages over their bearing equivalents, such as an absence of wear and friction, more customisable rigidity and no need for lubrication. Furthermore, they are more predictable when dynamics are a consideration. However, these factors come at the cost of a limited range of motion - due to the need to minimise stresses such that deflections are kept to the linear-elastic region. Incidentally, this allows their great repeatability and therefore, suitability for high precision engineering.

This report considers two linear flexure mechanisms: a leaf-spring and notch-hinge equivalent. Both consist of a platform, which is translated by deformation of spring members. The main difference being the member form, as shown in *Figure 1.* The notch-hinge lends itself better to monolithic manufacture and exhibits reduced buckling tendencies due to greater average member thickness. The leaf-spring is typically an assembly, with the springs clamped to the base and platform. The next chapter attempts to quantify such differences with respect to their motion errors, deflection range and stiffness.

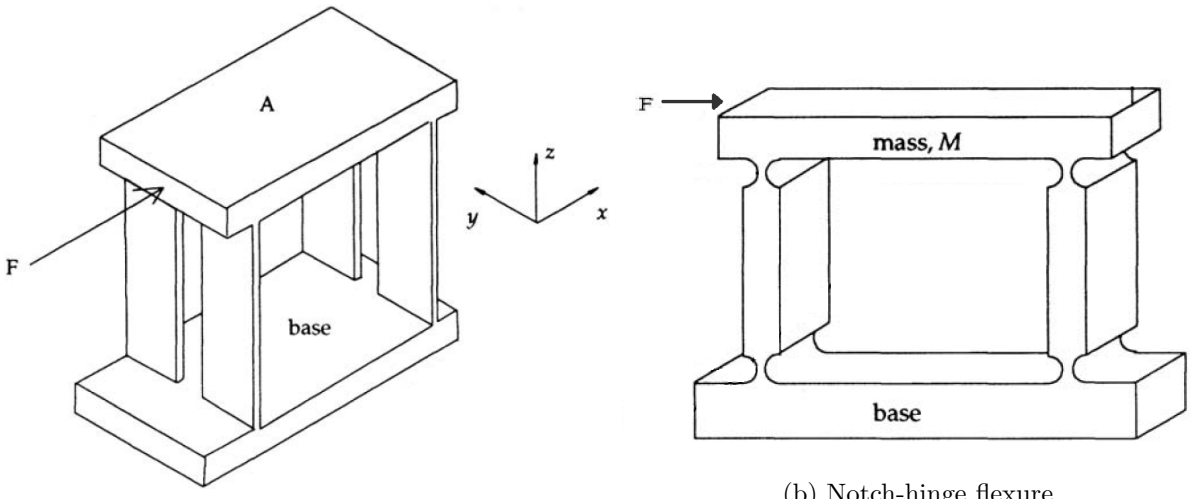

(a) Leaf-spring flexure

(b) Notch-hinge flexure

Figure 1: Varieties of simple linear flexure mechanisms (Smith & Chetwynd, 2005)

1 Mechanism design

1.1 Leaf-spring motion errors

This section details the characteristics and motion errors of a leaf-spring flexure. Of the latter, the two most prevalent are pitch error and vertical drift - due to dimensional tolerances and curvilinear error. These are minimised through optimisation of both machining processes and the proportions of the parameters below. Expressions for these are given in equations (1) & (2). Further errors may exist, including the variation of stiffness between members, another manufacturing concern due to the material structure and forming process used (i.e variation of stiffness due to the rolling direction of steel).

$$\theta_{pitch} = \left(\frac{6(l-2h)t^2}{3A^2l - 2t^2l + 6ht^2} \right) \qquad (1)$$

$$\delta_{vertical} \approx \frac{x^2}{2l} \qquad (2)$$

x = the horizontal distance moved by the flexure, l = spring length, t = spring thickness, A = platform length and h = the height of the driving force (from the base).

The extent of bending forces on the flexure may also result in error due to driving force misalignment. If this occurs at any point other than L/2 up the ligaments, the pitch error term (1) will be present. This point may, of course, be misaligned to begin with, if the members and platform are not perfectly parallel. Additionally, imperfect ligament clamping can effectively change the length of the members, resulting in slip and further misalignment. It is also worth considering that out-of-plane motion may exist due to a combination of all this, and the finite stiffness exhibited by the members in all other directions.

Given the repeatability of flexures, such errors are often systematic and are mitigated through calibration or servo nulling. Design adaptations may also achieve this, with one such measure being the use of a wobble pin for actuation. These increase the resolution with which the driving force is placed, thereby reducing force misalignment. Furthermore, careful ligament clamping, perhaps aided by Electrically Discharge Machined (EDM) hinges, may reduce slip, though at some financial cost. Lastly, the use of thin multi-blade ligaments is proven to increase the lateral stiffness and load capacity of leaf-springs, whilst keeping axial stiffness and stress concentrations relatively low. Further improvements may include the use of compound flexures or the use of symmetrical, suspended mechanisms. Of all these measures, some may prove more or less useful, depending on the specific context in which a flexure is required.

1.1.1 Leaf-spring design considerations

The following equations govern the ideal motion of a leaf-spring mechanism. The flexure stiffness λ in the direction of the driving force, is given by E the spring elastic modulus, I second moment of inertia and L length; the terms F and δ represent the driving force and resulting flexure deflection, respectively. I is dependent on length L, breadth b, thickness t as for a simple beam:

$$\lambda = \frac{F}{\delta} = \frac{24EI}{L^3} \qquad (3)$$

$$I = \frac{bt^3}{12} \qquad (4)$$

The maximum recommended limit for displacement is given in equation (5), where σ_{max} is one fifth of the spring yield strength, ensuring that only elastic behaviour occurs. This results in the desired, highly repeatable motion of a linear flexure. Equation (6) is concerned instead with their natural frequencies, as is important for a flexure's control and fatigue characteristics:

$$\delta_{max} = \frac{\sigma_{max} L^2}{3Ed} \qquad (5)$$

$$\omega_n = \left(\frac{\lambda}{M + \frac{2I}{L^2}} \right)^{1/2} \qquad (6)$$

The terms in (6) are M, the mass of the platform whilst I, L and λ remain as before. The resulting natural frequency is key in determining the mechanism's sensitivity to noise and an appropriate means of actuation. In summary, the parameters F, δ and ω_n represent the key design elements of a leaf-spring mechanism. These depend on a combination of geometric and material properties, which will be subject to further analysis in the following subsection.

1.1.2 (A) Aluminium leaf-spring flexure design

This subsection specifies the design of a leaf-spring mechanism through selection of the dimensions t, b and L and an appropriate choice of aluminium (Al) alloy. As equations (3-6) rely on the properties of yield strength, density and elastic modulus; the choice of alloy can, in particular, affect the displacement range considerably. This is strongly dependent on σ_{max} which varies with the hardness and temper of an alloy, ranging from 80 MPa for untempered 1050A alloy to 505MPa for solution-treated 7075 T6 alloy.

The latter was chosen for further analysis as it possesses one of the greatest ratios of σ_{max}/E of any commercial Al alloy (Kissel, 2005), despite a relatively high cost per unit volume. This ratio is key in enhancing flexure utility as range is typically the limiting factor. The lack of explicit cost or precision constraints therefore retains the focus towards achieving this objective.

Table 1: Chosen design parameters

Alloy	**Young Modulus (GPa)**	**Yield Strength (MPa)**	**Density (Kg/m^3)**
7075 (T6)	71.7	503	2810
Dimension (mm)	$\boldsymbol{t}$	$\boldsymbol{b}$	$\boldsymbol{L}$
-	0.898	8.313	60
$\boldsymbol{F_{drive}}$ **(N)**	δ_{max} **(mm)**	λ **(Nm^{-1})**	ω_n **(Hz)**
4.995	1.875	3996	556

For selection of t, b and L, equations (3-6) were iterated towards a target (maximum) deflection of 1.875mm and driving force of 5N. The former was chosen so as to provide a 50% safety factor over the design specification. For calculation of the driving force, equation (3) was solved for F by multiplying the right hand side by δ, which was taken to be 1.25mm. Full results describing the optimised flexure design are displayed in table (1) above. The values for F_{drive} and δ_{max} produced a variation of 0.1% and 0.005% respectively, from the aforementioned targets.

In determining the natural frequency, dimensions of 60 x 10 x 8 mm were used, along with the specified density, to provide a platform mass M of 12.91g. The ligaments were assumed to be of negligible mass with respect to the platform, as the latter represents the main component of inertia, throughout oscillations of the whole mechanism.

There are important practical implications to this set of design parameters; in particular, the breadth requires a manufacturing tolerance down to 100nm. This will necessitate the use of fine wire EDM fabrication, which will prove expensive. Fortunately, the other dimensions are less demanding and can be achieved with CNC mills (platform) or water-jet cutting (t & L).

1.1.3 (B) Notch-hinge flexure design

This subsection investigates the use of the alternative notch-hinge flexure. For consistent comparison with the leaf-spring, the same platform dimensions were used. The criteria for determining the stiffness and deflection of a notch-hinge mechanism are given by:

$$\lambda = \frac{\sigma E b t^3}{6KRL^2} \qquad (7) \qquad\qquad \delta_{max} = \theta_{max} L = \frac{4K}{K_t}\frac{RL}{Et}\sigma_{max} \qquad (8)$$

K, K_t = stress concentration factors, b = flexure breadth (as in **A**), $t = 0.5$mm notch thickness, $R = 2.5$mm notch radius, $L = 70$mm centre-to-centre notch distance.

These empirical stress concentration factors are dimensionless ratios of notch thickness : radius and are given below. These were calculated to be 0.2790 (K) and 1.0494 (K_t):

$$K = \frac{0.565t}{R} + 0.166 \qquad (9) \qquad\qquad K_t = \frac{2.7t + 5.4R}{8R + t} + 0.325 \qquad (10)$$

Upon application of equations (7-10) the resulting stiffness, deflection and natural frequencies were found to be 3.63MN/m, 0.1306 mm and 16.4kHz, respectively. When compared to the leaf-spring of similar dimensions, the notch-hinge exhibits a reduced range of motion. There are several implications of this, including the reduced allowable stress of the notch which is likely due to its greater localised stress concentrations. This makes sense, given that, in contrast, the stresses in deflection of the leaf-spring are distributed over the entire hinge (Awtar, 2004).

When considering between the use of the two, it is important to realise that each is a compromise. For this more-limited deflection, the notch-hinge possesses much higher off-axial stiffness and rotational precision. This will likely result in fewer parasitic motions, especially if coupled with monolithic and compound design. Careful consideration is needed of the exact application of such a flexure, particularly with regards to the compromise between stiffness and deflection.

The following analyses break away from this comparison and examine the effect of variations in material and geometry, specifically on the notch hinge mechanism. Table 2 shows the former, with the differing materials of 7075 alloy, AISI 304 stainless steel and Perspex acrylic polymer:

Table 2: Notch-hinge material variation

Material	δ_{max} **(mm)**	λ **(Nm^{-1})**	ω_n **(kHz)**
7075 (T6)	0.1306	3.63×10^6	16.7
AISI 304	0.0203	9.98×10^6	16.1
Perspex	0.4348	1.63×10^5	5.33

Evidently from the above, the choice of steel over Al results in a 3x increase in stiffness but with $1/6^{th}$ the deflection, however, the natural frequencies remain similar. The perspex flexure exhibits a greater range of deflection ($\sim$ 4x) but with nearly an order of magnitude in difference for stiffness. Note that the natural frequency is approximately $1/3^{rd}$ of the others. Careful consideration must clearly be made of material choice in designing flexures, especially with regards to variation of the three key parameters above.

The notch radius is a further parameter that can markedly affect the stiffness and deflection of a notch-hinge flexure. The following table examines the effect of varying R for the 7075 mechanism, whilst all other dimensions are as before:

Table 3: Notch-hinge radius variation

Radius (mm)	**0.5**	**1**	**2.5**	**5**	**10**
λ (MNm^{-1})	6.93	5.65	3.63	2.28	1.30
δ_{max} (mm)	0.0586	0.0787	0.1306	0.2302	0.3768

From table 3, it is clear that increases in notch radius result in reduced stiffness. This reduction appears to increase near-proportionately with R and corresponds to the effect of the bending moment on a reduced hinge profile. Conversely, the deflections are seen to increase with R in similar proportions. These relations serve to highlight the fundamental compromise between deflection and stiffness, that underpins flexure design.

1.1.4 (C) Geometric scaling of a leaf-spring flexure

This subsection attempts to highlight the implications of geometric scaling, applied to all the flexure dimensions (ligament & platform) in section A. Reduction factors of 10 and then 100 were chosen and the resulting δ_{max}, F_{drive}, λ and ω_n recorded below in table 4. It is immediately apparent that there is a corresponding 10x or 100x increase or decrease for each property, with none exhibiting any disproportionate effects. This may be expected, as such linear flexures reliably retain their behaviour down to nano-metre orders of magnitude (Lobontiu, 2002).

Table 4: leaf-spring geometric scaling effects

Scale Factor	δ_{max}	λ	F_{drive}	ω_n
1	1.875	3996	4.95	556
0.1	0.1875	399.6	0.495	5563
0.01	0.0188	39.96	0.0495	55630

1.1.5 (D) MEMS flexure mechanism

This subsection details the design and analysis of MEMS scale flexures of the type in section A. Equations (3), (4) and (5) were used to determine their deflection range, stiffness and natural frequency, whilst comparison was made between the use of polysilicon and silicon nitride. As evident in table 5, they present contrasting mechanisms with PolySi being twice as stiff yet with half the range of deflection of silicon nitride. Their natural frequencies are broadly similar.

Dimensions: Platform $= 200\mu\text{m}\times40\mu\text{m}\times5\mu\text{m} \parallel$ Ligaments $= b \sim 5\mu\text{m}, \text{L} \sim \text{D} \sim 200\mu\text{m}, \text{t} \sim 3\mu\text{m}$

Mechanical properties:
Silicon Nitride: $\rho = 3150\ kgm^{-3}$, E = 295 GPa, $\sigma_y = 3.012$ GPa
Polysilicon: $\rho = 2325\ kgm^{-3}$, E = 147.5 GPa, $\sigma_y = 3.330$ GPa

Table 5: MEMS Flexure Characteristics

Material	Max. Deflection (nm)	Stiffness (Nm^{-1})	Natural Frequency (MHz)
Silicon Nitride	4.54	9.96	0.28
Polysilicon	10.03	4.98	0.23

2 System fabrication

The manufacture of MEMS devices is often complex, tenuous and expensive. This section will outline some of the main methods by which they are produced, though further context for the mechanism will be needed for even a vaguely authoritative recommendation. A key further consideration is the actuation method as this heavily influences material, form and therefore fabrication of the mechanism.

Given that several thousands of the devices examined in section (D) are required, an appropriate means of fabrication may lie within the realms of micromachining. There are many reasons for this, the foremost being that this is the most established and reliable technique for the manufacture of micro mechanical structures (Gardner et al, 2001). The desired quantity represents a sizeable volume which, though not quite the heights of mass manufacture, constitutes a significant batch quantity. As silicon (Si) forming processes can be notoriously unpredictable, the aforementioned reliability is a highly desired attribute.

Micromachining broadly involves the formation of structures through material deposition, typically onto an Si wafer. This is followed by selective patterning onto a sacrificial layer, then deposition of the structural layer. Lastly, the sacrificial layer is etched away to reveal the intended structure. These processes are demonstrated in figure 2 below. Depending on the exact context, either bulk or surface micromachining may be most suitable. The use of Chemical-vapour deposition (CVD) is widely conducted and is compatible with polysilicon and silicon nitride, as in the mechanism outlined under part (D). Surface micromachined devices are typically limited to vertical dimensions of $\sim 2\mu m$ and require multiple stages to build structures (Gad-el-Hak, 2002). As those specified are up to 200 μm, bulk micromachining may be necessitated as it can extend to lengths of up to several wafer thicknesses or $\sim 300\mu m$, for MEMS level fabrication.

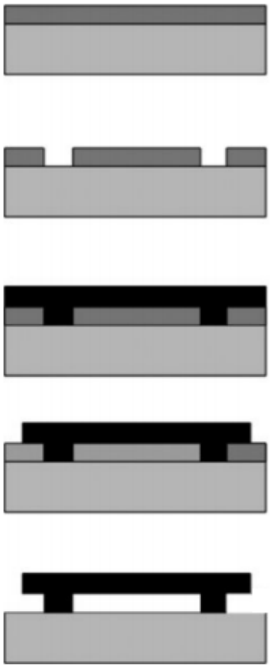

Figure 2: Micromachining process for flexure fabrication (Castaner, 2015)

Oxidation processes are generally avoided as the presence of silicon dioxide generates considerable stresses in the deposited films due to thermal expansion against the underlying silicon (Maluf, 2004). Moreover, the effect on cantilevers may be profound due to the subsequent warping this can cause. For these reasons, it is not recommended that SiO_2 be considered for flexure use though it may prove useful as an electrical insulator and under different mechanical configurations.

Figure 2 shows how an exact leaf-spring form may be obtained through surface micromachining. The base layer is the silicon substrate whilst the black one represents the structural layer. The other is the sacrificial layer used for etching.

References

Awtar, S. (2004). *Synthesis and analysis of parallel Kinematic XY flexure mechanisms*, PhD thesis, Dspace MIT.

Franssila, S. (2010). *Introduction to microfabrication*, John Wiley, Chichester.

Gardner, J. W. and Varadan, V. K. (2001). *Microsensors, MEMS and Smart Devices*, John Wiley & Sons, Inc., New York, NY, USA.

Hughes, I. and Hase, T. (2011). *Measurements and their uncertainties: a practical guide to modern error analysis*, Oxford University Press, Oxford.

Leach, R. K. and Smith, S. T. (2018). *Basics of precision engineering*, CRC Press, an imprint of Taylor & Francis, Boca Raton, FL, USA.

Li, S. and Yu, J. (2014). Design principle of high-precision flexure mechanisms based on parasitic-motion compensation, *Chinese Journal of Mechanical Engineering* **27**(4): 663-672.

Lobontiu, N. (2002). *Compliant Mechanisms: Design of Flexure Hinges*, 1 edn, CRC Press.

Mekid, S. (2008). *Introduction to Precision Machine Design and Error Assessment*, Mechanical & Aerospace Engineering Series, CRC Press.

Nadim Maluf, K. W. (2004). *An Introduction to MEMs Engineering*, 2 edn, Artech House Publishers.

Ryu, J. and Gweon, D. (1997). Error analysis of a flexure hinge mechanism induced by machining imperfection, *Precision Engineering* **21**(2): 83-89.

Smith, S. T. and Chetwynd, D. G. (2005). *Foundations of ultraprecision mechanism design*, Yverdon, Switzerland : Gordon and Breach Science Pub. Previous ed. published: 1992, 1994.

Sydenham, P. H. (1984). Elastic design of fine mechanism in instruments, *Journal of Physics E: Scientific Instruments* **17**(11): 922.

* All material properties used were obtained from the Cambridge-MIT MDP databook:
http://www-mdp.eng.cam.ac.uk/web/library/enginfo/cueddatabooks/materials.pdf